Reduction Behavior of the Early Actinyl Ions in Aqueous Solution

Valérie Vallet, Laurent Maron, Bernd Schimmelpfennig, Thierry Leininger,[†] Christian Teichteil,[†] Odd Gropen,[‡] Ingmar Grenthe,[§] and Ulf Wahlgren*

Institute of Physics, Stockholm University, P.O. Box 6730, S-11385 Stockholm, Sweden

Received: May 18, 1999

We investigate in this paper the reduction properties of the early actinyl ions. Geometry optimization and reaction energies were calculated at the correlated level, using effective core potentials. In a second step we included spin−orbit interaction calculated at the quasi-degenerate perturbation level. We report a general trend which is in agreement with experiment.

Introduction

Actinides are characteristic components in nuclear wastes, and in order to recycle these one needs to separate the different actinides. One property which can be used in the separation is the difference in their redox properties. Oxidation and reduction reactions are also important for the mobility of actinides in the groundwater system, a particular case of which is the integrity of spent nuclear fuel in contact with groundwater. Actinide(IV) compounds are very insoluble while most actinides(VI) are soluble, and immobilization would thus involve reduction of actinides from oxidation state VI to IV. In general transuranium(VI) complexes are more easily reduced than those of uranium.

From an experimental point of view, investigations of uranium compounds are straightforward, whereas for some of the transuranium elements, such as plutonium, high-level safety efforts are necessary. Thus, theoretical studies might support and guide the experimentalists in finding which reactions could be interesting for further investigations.

Several difficulties have to be overcome for an accurate theoretical treatment of actinides complexes. Relativistic effects have to be treated rigorously, and, as has been shown by Pyykkö,[1] the outer core in the early actinides is highly polarizable and must be considered as part of the valence shells.

Correlation effects are large in, for example, the actinyl(VI)-type complexes due to the high electronic density in the bond region.[2] Actinyl ions can coordinate many ligands[3] and a large number of electrons have to be treated explicitly. The diffuse character of the 5f-orbitals and the fact that actinyl compounds usually are not fully saturated lead both to high-spin multiplicities and pronounced spin−orbit effects from the open f-shells and an active participation of the f-orbital in the bonding.

Over the last years, several methods have been developed which in principle can deal with these problems; an overview of relativistic methods can be found in ref 4. However, due to the high computational demands, most of the explicit correlation treatments are restricted to moderately sized model systems. Alternatively density functional theory (DFT) methods, which are much less dependent on the number of electrons in the correlation treatment, can be used. Characteristic of the functionals used in DFT is that they usually are parametrized using properties of light elements, and their accuracy for heavier elements is unclear. So far, DFT methods or perturbation-type theories have been used with apparent success in a number of studies of geometries and binding energies for actinide complexes in a given oxidation state.[5−9] However, our experience is that DFT is less reliable in situations where the oxidation state is changed.[2]

Relativistic effective core potentials allow moderately large systems to be studied using multi-reference variational techniques. A systematic comparison of correlation approaches at both the all-electron and RECP levels has been reported elsewhere.[2]

In the present paper we present a systematic study of the reduction properties of the actinyl ions XO_2^{2+}, where X = U, Np, Pu, Am. We use the same model for the reduction, based on a two-step mechanism for the reduction involving $X^{(V)}$ as intermediate compound as proposed in ref 2.

During the first reaction, the actinyl ion is reduced from (VI) to (V) by adding one electron into an open f-shell:

$$XO_2^{2+} + \frac{1}{2}H_2O \rightarrow HOXO^{2+} + \frac{1}{4}O_2 \qquad (1)$$

In the second step, the actinide is further reduced to (IV) by adding a second f-electron:

$$HOXO^{2+} + \frac{1}{2}H_2O \rightarrow X(OH)_2^{2+} + \frac{1}{4}O_2 \qquad (2)$$

The global reaction can be written as follows:

$$XO_2^{2+} + H_2O \rightarrow X(OH)_2^{2+} + \frac{1}{2}O_2 \qquad (3)$$

The model reaction illustrated above is probably not realistic in itself, as the early actinyls(VI) are not reduced by water. However, the reactions may serve as prototypes for a reduction mechanism, and through the study of this model reaction for a whole sequence of early actinides, we may hope to improve the understanding of actinyl reduction in general. It is gratifying that our calculations adhere to the experimental knowledge that

* Author to whom correspondence should be addressed.

[†] Permanent address: Laboratoire de Physique Quantique, I.R.S.A.M.C, Université Paul Sabatier and CNRS (UMR 5626) 118, route de Narbonne, 31062 Toulouse cedex, France.

[‡] Permanent address: Institute of Mathematical and Physical Science, University of Tromsø, N-9037 Tromsø, Norway.

[§] Permanent address: Department of Chemistry, Inorganic Chemistry, The Royal Institute of Technology, Teknikringen 30, 10044 Stockholm, Sweden.

10.1021/jp991609t CCC: $18.00
Published on Web 10/30/1999

TABLE 1: Configurations of the Optimized Ground States

compound	ground state	configuration
UO_2^{2+}	$^1\Sigma_g^+$	f^0
$HOUO^{2+}$	$^2\Phi_u$	f_ϕ^1
$U(OH)_2^{2+}$	^3H_g	$f_\phi^1 f_\delta^1$
NpO_2^{2+}	$^2\Phi_u$	f_ϕ^1
$HONpO^{2+}$	^3H_g	$f_\phi^1 f_\delta^1$
$Np(OH)_2^{2+}$	$^4\Phi_u$	$f_\phi^1 f_\delta^2$
PuO_2^{2+}	^3H_g	$f_\phi^1 f_\delta^1$
$HOPuO^{2+}$	$^4\Phi_u$	$f_\phi^1 f_\delta^2$
$Pu(OH)_2^{2+}$	$^5\Sigma_g^+$	$f_\delta^2 + {}^1/_2 f(f_\phi^1 + f_\pi^1)$
AmO_2^{2+}	$^4\Phi_u$	$f_\phi^1 f_\delta^2$
$HOAmO^{2+}$	$^5\Sigma_g^+$	$(f_\phi^2 f_\delta^2)$
$Am(OH)_2^{2+}$	$^6\Pi_u$	$f_\phi^2 f_\delta^2 f_\pi^1$

the ease of reduction of actinyl ions increases along the series. In addition, our results clearly illustrate the stability of the oxidation state (V) for Np.

Computational Details

Energy-consistent small-core ECPs[10] and their corresponding optimized basis sets were used for the actinides and for oxygen. The basis sets of the actinides were improved by adding two g-functions. We also added two ANO-d-functions on oxygen. Hydrogen is described by the basis set suggested by Huzinaga[11] (5s) → [3s], using one additional p-function.

All the geometry optimizations were carried out using the MOLPRO 97.5 package.[12] Instead of the appropriate linear symmetry groups $C_{\infty v}$ and $D_{\infty h}$, we used the abelian sub-groups C_{2v} and D_{2h}, compatible by the package we use. Due to the lowering of symmetry and the use of real harmonics, the open f-shells, which are quite atom-like in all cases we have studied, couple to a high number of degenerate determinants which have to be treated simultaneously in a multi-configurational approach. The molecular orbitals were obtained in a RASSCF procedure by distributing 0−6 electrons in the seven atomic-like f-orbitals. Correlation effects were treated within the multi-reference AQCC scheme,[13] which includes a size-consistency correction. Optimized geometries were obtained using a gradient approach at this level of correlation.

The spin−orbit interaction was computed at the quasi-degenerate perturbation level using the CIPSO code.[14] The spin−orbit integrals were calculated within the atomic mean-field approach using the AMFI-code.[15] They were obtained in an all-electron basis set optimized by Faegri,[16] and the contraction coefficients were obtained according to the Raffeneti scheme using an atomic-SCF program including scalar relativity within the Douglas-Kroll formalism.[17] The integrals were merged with the ECP wave function using the one-to-one correspondence method proposed in ref 18. The spin−orbit calculations were carried out at the equilibrium distances using the *MOLCAS*-4 package[19] and the variational part of the CIPSI-code[20] for the correlation treatment. The spin−orbit matrix was set up by including all determinants in the f^n-manifold ($n = 1$, ..., 6). The diagonal elements of the spin−orbit matrix were shifted using the spin-free correlated energies calculated at the SDCI plus Davidson correction level, according to the technique proposed in refs 14, 21.

Results and Discussion

Geometries. The electron configurations of the spin-free optimized ground states are presented in Table 1. The $f_\sigma f_\pi$-orbitals correspond to molecular anti-bonding orbitals in which the main contribution comes from the atomic f-orbitals.

TABLE 2: Optimized Geometries for Actinyl Ions XO_2^{2+} at the AQCC Level[a]

actinyl ion XO_2^{2+}	R(X−O)	ΔR(X−O)	charge of X
UO_2^{2+}	1.7090	+0.0658	+2.57
NpO_2^{2+}	1.6933	+0.0654	+2.40
PuO_2^{2+}	1.6767	+0.0679	+2.33
AmO_2^{2+}	1.6246	+0.0314	+2.20

[a] ΔR is the difference between the optimized geometries at the correlated level (AQCC) and the RASSCF level. We also show the charge of the actinide atom obtained with Mulliken analysis at the AQCC level. Distances in Å.

The atomic character of the open-shell orbitals makes it reasonable to try to apply the atomic Hund's rule. This works well for the uranium compounds, but not, for example, for neptunium. The doubly reduced neptunyl ion $Np(OH)_2^{2+}$ is a $4\Phi_u$, whereas in an atomic case, it would have been a ^4I_u ($f_\phi^1 f_\delta^1 f_\pi^1$) (see Table 1). However, for all cases under investigation, we found the highest possible spin-coupling to be the ground state.

The optimized geometries obtained at the correlated level are shown in Tables 2, 3, and 4. In ref 2 we showed that, for uranyl and reduced uranyl, all-electron and RECP calculations are equivalent within chemical accuracy. In the present study we have therefore only used the comparably cheaper RECP method.

In Table 2, one can observe a shortening of the R(X−O) bond length along the actinyl(VI) series, by 0.08 Å from uranium to americium. This trend is expected from the decrease in atomic radius along the series. As the nuclear charge increases from uranium to americium, the 5f-orbitals tend to contract and the oxygen atom has to move closer to the actinide atom to form the bond.

We can analyze the effect of correlation on the bond by comparing the optimized bond lengths obtained at the RASSCF and correlated level (AQCC). For actinyl ions XO_2^{2+}, the correlation affects the bond significantly, leading to a lengthening of roughly 0.03−0.07 Å (cf Table 2). This can be explained by the nature of the bonding between the actinide atom and the oxygen. Actually, there is a strong interaction with the atomic $6d_\sigma$, $6d_\pi$, the σ and π 5f-orbitals of the actinide, leading to six orbitals which are prepared for two triple bonds: σ_g, σ_u, π_g, π_u.[1,2]

The bond lengthening due to correlation is similar for X = U, Np, Pu. However, the americyl ion shows a somewhat different behavior. The equilibrium distance is shorter than for the other ions, presumably due to the contraction of the 5f-orbital. We can guess that after americium, the 5f-orbitals are too contracted to participate in the bond. Actinyl ions would then not be stable anymore, which is in agreement with experiment.

All the singly reduced $HOXO^{2+}$ species show the same geometrical trend along the series (see Table 3). The effect of adding one hydrogen atom is a substantial lengthening of about 0.20 Å, of the bond between the actinide and the OH group (R(X−O_1) in Table 3). The bond between the actinide and the remaining oxygen (R(X−O_2)) is much less affected, as we report a change of 0.04 Å of the bond length. The lengthening of R(X−O_1) can be described as a bond-breaking process. In fact, when the hydrogen approaches one of the oxygen atoms to make a bond, the actinide−oxygen π_g bond of the actinyl ion breaks symmetrically. This means that we end up with one electron on the actinide which is of d-character, but goes finally to the 5f-orbital which is lower in energy. After electronic rearrangement on the oxygen atom, we end up with a σ bond between oxygen and hydrogen and a π-type lone-pair. Finally, we can summarize the electronic structure of the ion as a triple bond

TABLE 3: Optimized Geometries for the Singly Reduced Actinyl Ions $HOXO^{2+}$ at the AQCC Level[a]

$HOXO^{2+}$ ion	R(X−O1)	R(X−O2)	R(O2−H)	ΔR(X−O1)	ΔR(X−O2)	ΔR(O2−H)
$HOUO^{2+}$	1.7477	1.9179	0.9906	+0.0785	+0.0361	+0.0095
$HONpO^{2+}$	1.7143	1.8844	0.9869	+0.0685	+0.0346	+0.0180
$HOPuO^{2+}$	1.6975	1.8301	0.9879	+0.0745	+0.0164	+0.0164
$HOAmO^{2+}$						

[a] ΔR is the difference between the optimized geometries at the correlated level (AQCC) and the RASSCF level. Distances in Å.

TABLE 4: Optimized Geometries for the Doubly Reduced Actinyl Ions $X(OH)_2^{2+}$ at the AQCC Level[a]

$X(OH)_2^{2+}$ ion	R(X−O)	R(O−H)	ΔR(X−O)	ΔR(O−H)
$U(OH)_2^{2+}$	1.9910	0.9834	-0.0023	+0.0139
$Np(OH)_2^{2+}$	1.9270	0.9799	-0.0171	+0.0228
$Pu(OH)_2^{2+}$	1.9049	0.9784	-0.0423	+0.0218
$Am(OH)_2^{2+}$	1.9073	0.9937	-0.0197	+0.0251

[a] ΔR is the difference between the optimized geometries at the correlated level (AQCC) and the RASSCF level. Distances in Å.

TABLE 5: Comparison of Reaction Energies with and without Spin−Orbit Effects for the First Step of the Reduction Mechanism

	RECP	
compounds	spin-free (AQCC)	with spin−orbit
uranyl UO_2^{2+}	10.61	3.91
neptunyl NpO_2^{2+}	−12.93	−19.56
plutonyl PuO_2^{2+}	−3.43	−5.87
americyl AmO_2^{2+}	−34.29	−36.17

[a] Energies in kcal mol^{-1}.

TABLE 6: Comparison of Reaction Energies with and without Spin−Orbit Effects for the Second Step of the Reduction Mechanism[a]

	RECP	
compounds	spin-free (AQCC)	with spin−orbit
uranyl UO_2^{2+}	5.57	-1.38
neptunyl NpO_2^{2+}	8.23	5.03
plutonyl PuO_2^{2+}	−2.06	−4.17
americyl AmO_2^{2+}	−12.98	−18.56

[a] Energies in kcal mol^{-1}.

between the actinide atom and one of the oxygens and a double bond to the other one, but this picture is of course extremely simplified. The bond is partly covalent, partly ionic, although it should be emphasized that according to our results the covalent contribution is quite important. There is no significant change in the (O−H) distance.

In the second step of the reduction reaction, the $HOXO^{2+}$ ion is reduced to the symmetric ion $X(OH)_2^{2+}$. The mechanism is similar to the one described above. The remaining triple bond in the singly reduced ion is broken and the final electronic structure has, using the same picture as above, two double X−O bonds and two O−H bonds.

Reaction Energies. Tables 5, 6, and 7 show the energies of the first and second steps of the reduction mechanism, and for the global reaction.

Let us start by considering the reduction of uranyl(VI). This reaction has been studied previously both at the all-electron and the ECP levels, and using a variety of correlation methods.[2] One of the findings in that study was that there were virtually no differences between the all-electron and the ECP results, and we are therefore confident that our present results are reliable.

For uranyl both steps in the reaction are endothermic at the spin-free level, making the full reaction endothermic by 16.2 kcal mol^{-1} (Figure 1). Since all spin−orbit calculations were done at the perturbation level in the f-manifold, the second-order spin−orbit effects are neglected. The closed-shell uranyl-(VI) ion is thus not affected, and the spin−orbit effect lowers the energies of the products and thus the reaction energies. The first reaction becomes less endothermic by 6.7 kcal mol^{-1}, from 10.6 to 3.9 kcal mol^{-1}, and the second reaction, which was endothermic by 5.6 kcal mol^{-1}, becomes exothermic by 1.4 kcal mol^{-1}. The spin−orbit effect is thus substantial, and, as expected, larger for the first step than for the second step, due to the closed-shell character of uranyl(VI). The full reaction is still endothermic by 2.8 kcal mol^{-1} after spin−orbit effects have been accounted for. However, the spin−orbit effect is very large, reducing the reaction energy by 13.4 kcal mol^{-1}, and clearly cannot be neglected.

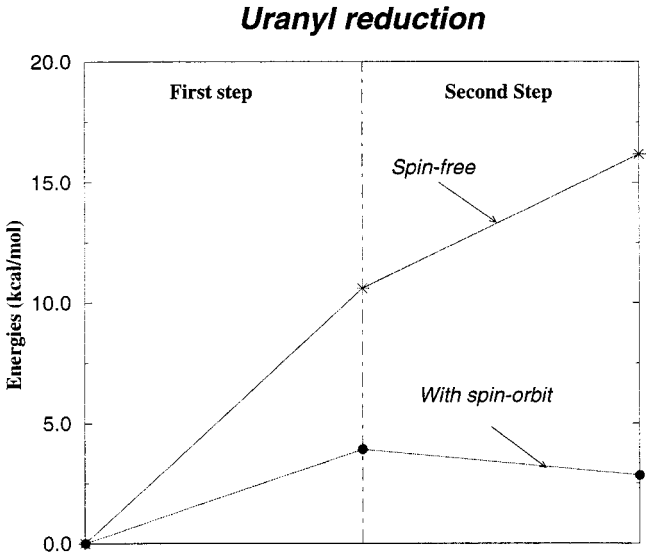

Figure 1. Influence of spin−orbit interaction on the uranyl reduction. Energies in kcal mol^{-1}.

Neptunium behaves somewhat differently. The first reaction is exothermic by 12.9 kcal mol^{-1} at the spin-free level. The effect of spin−orbit coupling on the reaction energy is almost as important as in the uranyl case, making the reaction exothermic by 19.6 kcal mol^{-1}. The second reaction is actually endothermic by 8.2 kcal mol^{-1} at the spin-free level by 5.0 kcal mol^{-1} as the spin−orbit level. This result clearly illustrates the well-known stability of neptunium(V).[3]

For plutonyl, the first reaction is exothermic by 3.4 kcal mol^{-1} at the spin-free level and 5.9 kcal mol^{-1} at the spin−orbit level, which is much less than for neptunyl. The second reaction, contrary to both uranyl and neptunyl, is also exothermic by 2.1 kcal mol^{-1} and 4.2 kcal mol^{-1} at the spin-free and spin−orbit levels, respectively. Americyl shows the same behavior as plutonyl, with the difference that the reaction is much more exothermic.

It is gratifying that our results so far are in agreement with experiment. The stability of neptunium(V) is clearly demonstrated, and the well-known fact that the heavier actinide(VI) ions are more easily reduced than the lighter ones is illustrated

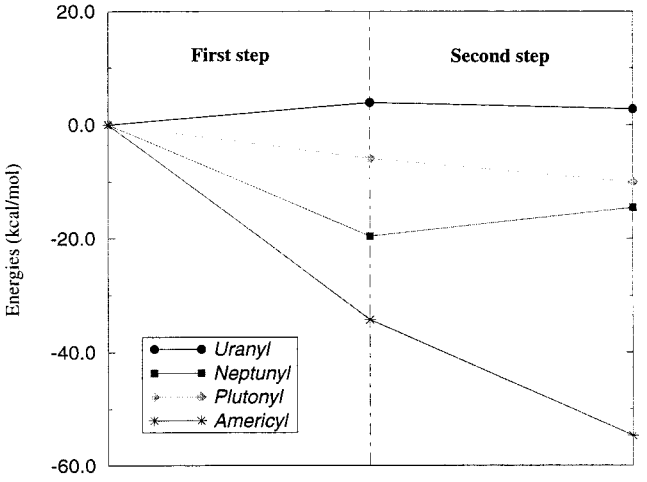

Figure 2. Reduction energetics of the actinyl ions in solution including spin−orbit effect. Energies in kcal mol^{-1}.

by the sequence uranyl, plutonyl, and americyl where both the individual and the global reactions go from endothermic for uranyl to strongly exothermic for americyl, with plutonyl in the middle.

It is noteworthy that the spin−orbit effect is very important for the uranyl and neptunyl reactions, but less so for plutonyl and americyl. The smallest effect occurs for plutonyl, and this can be explained by a change in the ground-state character of the doubly reduced plutonyl $Pu(OH)_2^{2+}$. At the spin-free level, the ground state is a $^5\Sigma_g^+$, whereas it is the $\Omega = 2$-component of the $^5\Gamma_g$ when the spin−orbit interaction is included. The latter state was lying 4 kcal mol^{-1} above the ground state at the spin-free level.

When the bond length decreases from 1.71 in UO_2^{2+} to 1.62 in AmO_2^{2+}, the charge on the actinyl center decreases monotonically from 2.57 on U to 2.20 on Am, see Table 2 (Figure 2). As the bond length gets shorter, the overlap between the valence orbitals increases and the electrons become more delocalized. This can be interpreted as an increased covalency in the bonds. A more detailed study of the bonding properties of actinide and lanthanide complexes is planned.

Comparison with Experiment. It is of interest to compare the theoretical reaction energies with experimental redox data in aqueous solution. This requires an estimate of the Gibbs energies for the transfer from the gas phase at 0 K to an aqueous solution at 298 K. Current theoretical methods are not accurate enough to make such estimates, and we have therefore estimated this quantity using the uranium system and the following thermodynamic cycle:

$$\begin{array}{ccccccc} UO_2^{2+}(g, 0\ K) & + H_2O\ (g, 0\ K) & \xrightarrow{\Delta U} & {}^{(1)}U(OH)_2^{2+}(g, 0\ K) & + & \frac{1}{2}O_2(g, 0\ K) & (4) \\ \downarrow & \downarrow & & \downarrow & & \downarrow & \\ UO_2^{2+}(aq, 298\ K) & + H_2O\ (aq, 298\ K) & \xrightarrow{\Delta G^\circ} & {}^{(2)}U(OH)_2^{2+}(aq, 298\ K) & + & \frac{1}{2}O_2(aq, 298\ K) & (5) \end{array}$$

The vertical arrows denote the solvation and temperature change reactions. Denoting the sum of these Gibbs energy changes $\Delta G°$(hydr) we obtain

$$\Delta G°(2) = \Delta U(1) + \Delta G°(\text{hydr})$$

We can now use the experimental value of $\Delta G°(2)$ and the theoretical value of $\Delta U(1)$ including spin−orbit coupling (Table 7) to estimate $\Delta G°$(hydr) for uranium.

TABLE 7: Comparison of Reduction Energetics with and without Spin−Orbit Effects for Actinyls in Aqueous Solution[a]

	RECP	
compounds	spin-free (AQCC)	with Spin−Orbit
uranyl UO_2^{2+}	16.18	2.83
neptunyl NpO_2^{2+}	−4.69	−14.53
plutonyl PuO_2^{2+}	−5.49	−10.04
americyl AmO_2^{2+}	−47.28	−54.74

[a] Energies in kcal mol^{-1}.

TABLE 8: Standard Gibbs Energies of Formation for Species in Reaction 5[a]

chemical species	$\Delta G^f(2)$
H_2O(I)	−56.60
UO_2^{2+} (aq)	−227.34
U^{4+}(aq)	−126.46
$U(OH)_2^{2+}$	−243.26

[a] Energies in kcal/mol.

TABLE 9: Thermodynamic Data for Reaction 6[a]

species	$\Delta G°$
Np	19.72
Pu	24.20
Am	−20.45

[a] Energies in kcal/mol.

The experimental $\Delta G°(2)$ was calculated from the Gibbs energies of formation given in Table 8, where the value for $U(OH)_2^{2+}$(aq) is estimated by us from the equilibrium constant at zero ionic strength for the reaction

$$U^{4+}(aq) + 2H_2O \rightleftharpoons U(OH)_2^{2+}(aq) + 2H^+(aq), \quad \log K = -2.65$$

using the experimental data from Grenthe et al.[22] in a 3 M perchlorate medium. The other Gibbs energies of reaction are taken from Grenthe et al.[23]

From these data we obtain $\Delta G°(2) = 40.67$ kcal/mol, and thus $\Delta G°(\text{hydr}) = 37.91$ kcal/mol.

Assuming $\Delta G°$(hydr) and the equilibrium constant for the hydrolysis reaction

$$M^{4+}(aq) + 2H_2O \leftrightarrow M(OH)_2^{2+}(aq) + 2H^+(aq)$$

to be constant along the series U → Am we can obtain estimates of $\Delta G°(2)$ for Np, Pu, and Am from the corresponding theoretical $\Delta U(1)$ values using $\Delta G°$(hydr) for uranium.

The Gibbs energies of reaction thus obtained for

$$MO_2^{2+}(aq) + 2H^+(aq) \rightarrow M^{4+}(aq) + H_2O + \frac{1}{2}O_2\ (g, f = l\ atm) \quad (6)$$

are given in the second column of Table 9. By combining eq 6 with

$$H_2O(1, 298\ K) \rightarrow H_2(g, f = 1\ atm) + \frac{1}{2}O_2(g, f = 1\ atm)$$

we obtain the standard Gibbs energy of reaction for the cell reaction in

TABLE 10: Thermodynamic Data for Reaction 7[a]

species	$\Delta G°(2)$	$E°_{6/4}$ theoretical	$E°_{6/4}$ experimental
Np	−36.40	0.80	0.84
Pu	−32.39	0.70	0.90
Am	−77.05	1.67	1.25

[a] Energies in kcal/mol, $E°_{6/4}$ in V.

$$+\mathrm{Pt}\left|\begin{matrix}\mathrm{H^+(a=1)}\\ \mathrm{H_2\ (g,f=1\ atm)}\end{matrix}\right|\left|\begin{matrix}\mathrm{UO_2^{2+}}(a=1)\\ \mathrm{U^{4+}}(a=1)\end{matrix}\right|\mathrm{Pt^-}$$

i.e.

$$\mathrm{MO_2^{2+}(aq,}\ a=1) + 2\mathrm{H^+}\ (\mathrm{aq,}\ a=1) + \mathrm{H_2(g,}\ f=\mathrm{l}) \rightarrow \mathrm{M^{4+}(aq,}\ a=1) + 2\mathrm{H_2O} \quad (7)$$

In eq 7 we have $\Delta G° = -2F.E°_{6/4}$, where $E°_{6/4}$ is the standard redox potential of the couple $\mathrm{MO_2^{2+}/M^{4+}}$. F is the Faraday constant. Theoretical and experimental values of $E°_{6/4}$ are given in Table 10.

The data in Table 10 give an indication of the differences to expect between experiments and theoretical calculations when using the crude approximation described above. A major cause for the differences between experiments and theory may be variations in the Gibbs energy of solvation along the actinide series. One part of our research program is to calculate the energy changes for reactions of the type

$$\mathrm{M^{4+}} + n\mathrm{H_2O} \rightarrow \mathrm{M(H_2O)_n^{4+}}$$

which may give some indication of the solvation energies and their variation along the actinide series.

Conclusion

The aim of the present paper was to study the reduction behavior of actinide(VI) ions in solution. As a first attempt, we considered a relatively simple gas-phase model only. We obtained an overall agreement with the experimental trend that the oxidation ability of actinyl ions increases in the sequence uranium to americium. However, the neptunyl shows a different behavior, which corresponds to the experimental knowledge that neptunium(V) is the most stable oxidation state in solution.

We have also demonstrated that the inclusion of spin−orbit interaction is very important in order to obtain a qualitative prediction of the energetic of the reduction reactions.

Acknowledgment. We thank Dr. W. Küchle and Dr. M. Dolg for providing unpublished basis sets. This work was supported by Grant No. V6414 from the Norwegian VISTA foundation. L.M. and V.V. are grateful to participate in the program of "cotutelle de Thèse" financed by the French government. B.S. thanks the Deutsche Forschungsgemeinschaft and the Norwegian Research Council for financial support. We also acknowledge the REHE program of the ESF for providing collaborations and promote quantum relativistic studies. This work has received support from The Research Council of Norway (Program of Supercomputing) through a grant of computing time.

References and Notes

(1) Pyykkö, P.; Li, J.; Runeberg, N. *J. Phys. Chem.* **1994**, *98*, 4809.
(2) Vallet, V.; Schimmelpfennig, B.; Maron, L.; Teichteil, Ch.; Leininger, Th.; Grenthe, I.; Wahlgren, U. *Chem. Phys*., **1999**, *244*, 185.
(3) Katz, J. J.; Morss, G. T.; Seaborg, L. R. *The Chemistry of Actinide Elements.* Vol 1; Chapmann and Hall: New York, 1986.
(4) Almöf, J. E.; Gropen, O. *Rev. Comp. Chem.* **1996**, *8*, 203.
(5) Ismail, N.; Heully, J-L.; Saue, T.; Daudey, J-P.; Marsden, C. J. *Chem. Phys. Lett.* **1999**, *300*, 296.
(6) Gagliardi, L.; Willets, A.; Skylaris, C-K.; Handy, N. C.; Spencer, S.; Ioannou, A. G.; Simper, A. M. To be published.
(7) Craw, J. S.; Vincent, M. A.; Hillier, I. H.; Wallwork, A. L. *Phys. Chem.* **1995**, *99*, 10181.
(8) Wahlgren, U.; Moll, H.; Grenthe, I.; Schimmelpfennig, B.; Maron, L.; Vallet, V.; Gropen, O. *J. Phys. Chem. A*, **1999**, *103*, 8257.
(9) Schrekenbach, J.; Hay, P. J.; Martin, R. L. *Inorg. Chem.* **1998**, *37*, 4442.
(10) Küchle, W.; Dolg, M.; Stoll, H.; Preuss, H. *J. Chem. Phys.* **1994**, *100* (10), 7535.
(11) Huzinaga, S. *J. Chem. Phys.* **1965**, *42*, 1293.
(12) *MOLPRO* is a package of ab initio programs written by Werner, H. J.; Knowles, J.; with contribution from Almlöf, P. J.; Amos, R. D.; Berning, A.; Deegan, M. J. O.; Eckert, F.; Elbert, S. T.; Hampel, C.; Lindh, R.; Meyer, W.; Nicklass, A.; Peterson, K.; Pitzer, R.; Stone, A. J.; Taylor, P. R.; Mura, M. E.; Pulay, P.; Schütz, M.; Stoll, H.; Thorsteinsson, T.; Cooper, D. L.
(13) Szalay, P. G.; Bartlett, R. J. *Chem. Phys. Lett.* **1993**, *214*, 481.
(14) Teichteil, Ch.; Spiegelmann, F. *Chem. Phys.* **1983**, *81*, 283.
(15) Schimmelpfennig, B. *AMFI, an Atomic Mean-Field Integral program*; Stockholm University, 1996.
(16) Faegri, K. Oslo University, private communication.
(17) Hess, B. A. *Phys. Rev. A* **1986**, *33*, 3742.
(18) Schimmelpfennig, B.; Maron, L.; Wahlgren, U.; Teichteil, Ch.; Fagerli, H.; Gropen, O. *Chem. Phys. Lett.* **1998**, *286*, 267.
(19) *MOLCAS*-4 *program package*; Andersson, K.; Blomberg, M. R. A.; Fülscher, M. P.; Karlström, G.; Lindh, R.; Malmqvist, P-Å.; Neogrády, P.; Olsen, J.; Roos, B. O.; Sadlej, M.; Schütz, A. J.; Seijo, L.; Serrano-Andrés, L.; Siegbahn, P. E. M.; Widmark, P.-O. Lund University, Sweden, 1997.
(20) Huron, B.; Malrieu, J. P.; Rancurel, P. *J. Chem. Phys.* **1973**, *58*, 5745.
(21) Schimmelpfennig, B.; Maron, L.; Wahlgren, U.; Teichteil, Ch.; Fagerli, H.; Gropen, O. *Chem. Phys. Lett.* **1998**, *286*, 261.
(22) Grenthe, I.; Bidoglio, G.; Omenetto, N. *Inorg. Chem.* **1989**, *28*, 71.
(23) Grenthe, I.; Fuger, J.; Konings, R. J. M.; Lemire, R. J.; Muller, A. B.; Nguyen-Trung, C.; Wanner, H. *Chemical Thermodynamics of Uranium*; North-Holland, 1992.